Geologica Acta, Vol.14, Nº 1, March 2016, 1-12
DOI: 10.1344/GeologicaActa2016.14.1.1

geologica acta

# Ca/Al of plagioclase-hosted melt inclusions as an indicator for post-entrapment processes at mid-ocean ridges?

H.T. ZHANG[1] Y.M. YANG[1,2,3*] Q.-S. YAN[1,2] X.-F. SHI[1,2] Z.-W. ZHU[1] W.-C. SU[4] C.-J. QIN[4] J. YE[1, 2]

[1]**Key Laboratory of Marine Sedimentology and Environmental Geology, First Institute of Oceanography, State Oceanic Administration**
Qingdao, Shandong 266061 China. Zhang E-mail: zht@fio.org.cn Zhu E-mail: zwzhu@fio.org.cn

[2]**Function Laboratory for Marine Geology, National Oceanography Laboratory**
Qingdao, Shandong 266071China. Yan E-mail: yanquanshu@163.com Shi E-mail: xfshi@fio.org.cn Ye E-mail: yejun@fio.org.cn

[3]**National Deep Sea Center, State Oceanic Administration**
Qingdao, Shandong 266061 China. Yang E-mail: yym@ndsc.org.cn

[4]**State Key Laboratory of Ore Deposit Geochemistry, Institute of Geochemistry, Chinese Academy of Sciences**
Guiyang, Guizhou 550002 China. Su E-mail: suwenchao@vip.gyig.ac.cn Qin E-mail: qinchaojian@vip.gyig.ac.cn

*Corresponding author

## ABSTRACT

The composition of melt inclusions in basalts erupted at mid-ocean ridges may be modified by post-entrapment processes, so the present composition of melt inclusions may not represent their original composition at the time of entrapment. By combining the melt inclusion composition in samples from the South Mid-Atlantic Ridge at 19ºS analyzed in this study, and from the Petrological Database, we found that post-entrapment crystallization processes resulted in higher Ca/Al, Mg#[100×atomic $Mg^{2+}/(Mg^{2+}+Fe^{2+})$], MgO and FeO contents, and lower CaO and $Al_2O_3$ contents of plagioclase-hosted melt inclusions relative to those hosted in olivine. In addition, melt inclusions hosted in plagioclase with anorthite content larger than 80mol.% had been modified more readily than others. By discussing the relationships between Ca/Al and fractional crystallization, post-entrapment crystallization, and the original melt composition, we propose that Ca/Al can be regarded as an indicator of the effect of post-entrapment processes on melt inclusion composition. Specifically, i) when Ca/Al<0.78, melt inclusion compositions corrected for fractional crystallization to Mg#=72 can represent the primary magma at mid-ocean ridges; ii) when 0.78<Ca/Al<1.0, melt inclusions are mainly modified by post-entrapment crystallization effects, and can reveal the original melt composition after correcting for these effects; iii) when Ca/Al>1.0, the compositions of melt inclusions do not reflect the original melt composition nor preserve information about the mantle source. According to these criteria, plagioclase-hosted melt inclusions with Ca/Al>1.0 in basalts from the South Mid-Atlantic Ridge at19ºS cannot represent the composition of the melt at the moment of their entrapment.

***KEYWORDS*** **Melt inclusions. Plagioclase. Ca/Al. Post-entrapment crystallization. South Mid-Atlantic Ridge 19ºS.**

## INTRODUCTION

Many previous studies on melt inclusions in Anorthite (An)-rich plagioclase in Mid-Ocean Ridge Basalt (MORB) samples focused on the nature of primitive MORB melts, and their interaction with residual mantle and crystal-rich cumulates (Dungan and Rhodes, 1978; Sinton *et al.*, 1993; Nielsen *et al.*, 1995; Kamenetsky *et al.*, 1998; Shimizu, 1998; Sours-Page *et al.*, 1999, 2002; Hansen and Gronvold, 2000; Lund, 2003; Danyushevsky *et al.*, 2003, 2004; Laubier *et al.*, 2007; Font *et al.*, 2007). The composition of these melt inclusions has generally larger uncertainties than that of bulk rock powder or basaltic glass, in terms of what it truly represents (Kent, 2008). The effects of chemical fractionation in the evolving host magma (Faure and Schiano, 2005; Baker, 2008), of Post-Entrapment Crystallization (PEC) (Danyushevsky *et al.*, 2000) and of melt inclusions' re-equilibration with the host crystal and/or external melt (Qin *et al.*, 1992; Danyushevsky *et al.*, 2000; Gaetani and Watson, 2000; Cottrell *et al.*, 2002; Spandler *et al.*, 2007; Portnyagin *et al.*, 2008; Neave *et al.*, 2013, 2014) on the melt inclusions composition may imply that the latter does not always represent the composition of the melt at the time of its entrapment.

Plagioclase phenocrysts may contain large numbers of melt inclusions, which may provide some important information on magmatic processes, for the diversity of compositions occurring in MORB magma systems. However, there is still debate on the ability of plagioclase to preserve the original composition of parent magmas (Cottrell *et al.*, 2002; Danyushevsky *et al.*, 2002). In addition, after being trapped, the composition of melt inclusions may be controlled by the composition of the host phenocryst during the PEC process (Tait, 1992). Therefore, the direct application of our understanding of macro-scale magmatic processes to the interpretation of melt inclusion data may result in some erroneous conclusions (Danyushevsky, 2002; Baker, 2008).

Post-entrapment processes in plagioclase-hosted melt inclusions can be identified and reversed through laboratory heating or numerical treatments which rely on too many assumptions (Hartley and Thordarson, 2013; Hartley *et al.*, 2013; Neave *et al.*, 2015). In a pioneer work by Font *et al.* (2007) aimed at revealing the original composition, the Ca/Al in all plagioclase-hosted melt inclusions was less than 1.0. This feature suggests that only the composition of melt inclusions with Ca/Al<1.0 has petrological significance. This attractive peculiarity, however, has not received much attention yet. This study aims at developing a new method for effectively identifying the melt inclusion composition modified by PEC or other more complex processes, avoiding complex and empirical composition restoring processes. We analyzed plagioclase-hosted melt inclusions in MORB samples from the South Mid-Atlantic Ridge at 19ºS area (SMAR19ºS), and combined the results with the composition of plagioclase- and olivine-hosted melt inclusions taken from the Petrological Database (PetDB, Lehnert *et al.*, 2000) to demonstrate that Ca/Al is an effective indicator to assess melt inclusion composition at the time of entrapment.

## SAMPLES AND METHODS

The SMAR19ºS segment is located southwest of the Saint Helena volcanic arc and offset by the Martin Vaz transform (Fig.1), and characterized by a half-spreading rate of about 17.9mm/year (De Mets *et al.*, 1994). During the China Ocean Survey (COS) Expedition nº. 22, MORB samples were collected at various sites located from 19.34ºS to 19.57ºS in the South Mid-Atlantic Ridge. The plagioclase phenocrysts in these basalts contain abundant ~20 to ~50µm-sized melt inclusions round or elliptical in shape.

Major element analyses of melt inclusions and host plagioclase phenocrysts were obtained by Electron-Probe Micro-Analysis (EPMA) (model: SHIMADZU EPMA-1600, made in Japan) at the State Key Laboratory of Ore Deposit Geochemistry of the Institute of Geochemistry, Chinese Academy of Sciences. The analytical method for determining the major oxide content of melt inclusions and plagioclase phenocrysts was as follows. First, a plagioclase phenocryst (size>0.2cm) containing a number of inclusions was polished to expose the inclusions at an arbitrary level (Danyushevsky *et al.*, 2004). Second, homogeneous melt inclusions (size>20µm) were analyzed with BackScattered Electron (BSE) images. The spatial resolution of the basaltic glass analyses was from <10 to ~20µm. Elements typically present in low abundances (*e.g.*, Cr, Mn, Ni, K, P, Cl, S, F) were difficult to measure precisely, being the analytical uncertainties on the order of ±10 to ±~50%. In order to obtain more accurate data, melt inclusions and plagioclases were analysed with an accelerating voltage of 25kV, a beam current of 10nA and a spot size of 5µm to minimize Na mobilization. Counting times were as follows: 20s for major oxides in glass and crystals, except for Ti that was counted for 60s, and Na that was counted for 10s. Calibration standards were as follows: jadeite for Na, periclase for Mg, Si glass for Si, K-feldspar for K, rutile for Ti, fayalite for Fe, corundum for Al, apatite for P, and pure metals for Cr, Mn and Ni. Repeated analyses of internal standards, *e.g.*, olivine, clinopyroxene and anorthite (GB/T 145075-94), indicate that major oxides (>1.0wt.%) and anorthite plagioclase content [An= 100×atomic Ca/(Ca+Na+K)] were determined with a precision of 1σ= ±0.5wt.% and 1σ= ±0.5mol.%, respectively. In this study a comparison between host plagioclase crystal's composition

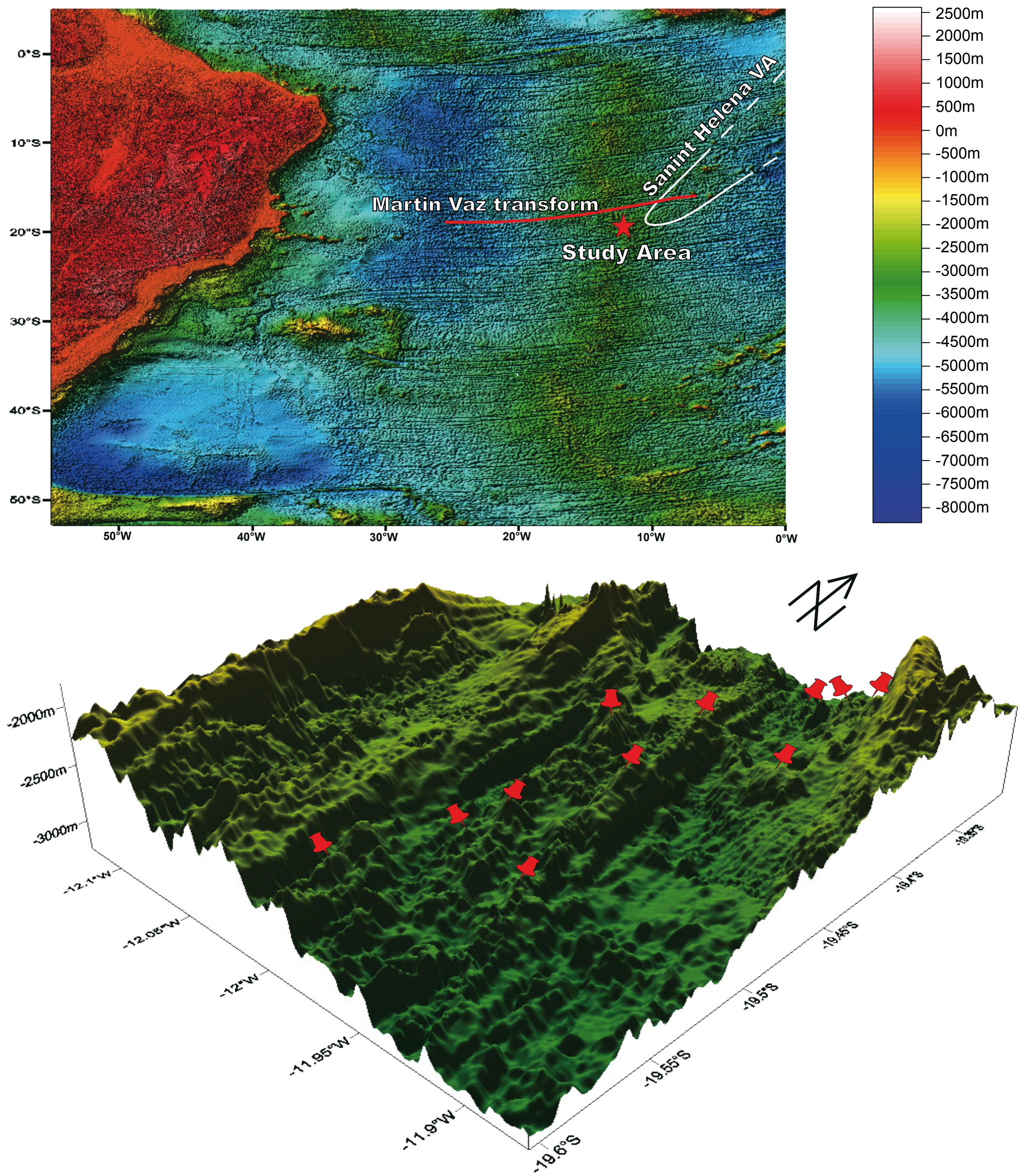


**FIGURE 1.** Up: Location (red star) of the study area in the South Mid-Atlantic Ridge; Down: multi-beam image of the South Mid-Atlantic Ridge at 19°S and sampling sites (red caps).

**TABLE 1.** Major element composition of plagioclase-hosted melt inclusions in SMAR19ºS MORB (wt.%)

| Sample | MI1 | MI2 | MI3 | MI4 | MI5 | MI6 | MI7 | MI8 | MI9 | MI10 | MI11 | MI12 |
|---|---|---|---|---|---|---|---|---|---|---|---|---|
| | Pl12 | Pl13 | Pl14 | Pl11 | Pl14 | Pl9 | Pl5 | Pl13 | Pl14 | Pl10 | Pl7 | Pl4 |
| $SiO_2$ | 51,38 | 50,66 | 50,94 | 50,95 | 47,63 | 50,20 | 50,51 | 49,06 | 50,05 | 51,13 | 48,36 | 48,56 |
| $TiO_2$ | 0,92 | 0,92 | 1,02 | 0,73 | 2,51 | 0,94 | 0,80 | 1,10 | 0,73 | 0,70 | 2,26 | 2,20 |
| $Al_2O_3$ | 7,14 | 5,82 | 6,40 | 7,10 | 6,38 | 6,93 | 5,83 | 5,73 | 6,82 | 9,06 | 4,76 | 6,28 |
| FeO | 14,57 | 14,81 | 14,46 | 13,37 | 16,07 | 13,38 | 14,10 | 14,15 | 13,87 | 12,88 | 15,95 | 14,23 |
| MgO | 13,71 | 14,53 | 14,09 | 14,96 | 13,68 | 14,28 | 15,01 | 14,98 | 14,35 | 13,43 | 16,54 | 15,30 |
| MnO | 0,26 | 0,29 | 0,25 | 0,23 | 0,30 | 0,25 | 0,28 | 0,24 | 0,25 | 0,21 | 0,28 | 0,25 |
| CaO | 10,77 | 10,79 | 10,95 | 11,43 | 10,87 | 11,46 | 11,49 | 12,05 | 11,53 | 11,50 | 11,70 | 11,20 |
| $Na_2O$ | 0,71 | 0,44 | 0,35 | 0,43 | 0,96 | 0,67 | 0,46 | 0,46 | 0,34 | 1,20 | 0,37 | 0,62 |
| $K_2O$ | 0,10 | 0,12 | 0,12 | 0,09 | 0,11 | 0,98 | 0,09 | 0,05 | 0,11 | 0,06 | 0,09 | 0,09 |
| $Cr_2O_3$ | 0,10 | 0,11 | 0,11 | 0,11 | 0,05 | 0,09 | 0,12 | 0,15 | 0,10 | 0,19 | 0,13 | 0,08 |
| NiO | - | 0,01 | - | 0,01 | 0,03 | 0,01 | 0,02 | 0,02 | 0,01 | 0,01 | 0,01 | - |
| Total | 99,66 | 98,50 | 98,69 | 99,41 | 98,59 | 99,19 | 98,71 | 97,99 | 98,16 | 100,37 | 100,45 | 98,81 |
| Ca/Al[1] | 1,51 | 1,85 | 1,71 | 1,61 | 1,70 | 1,65 | 1,97 | 2,10 | 1,69 | 1,27 | 2,46 | 1,78 |
| Mg#[2] | 0,65 | 0,66 | 0,66 | 0,69 | 0,63 | 0,68 | 0,68 | 0,68 | 0,67 | 0,67 | 0,67 | 0,68 |
| $Ca_{72}/Al_{72}$ | 1,25 | 1,53 | 1,42 | 1,44 | 1,35 | 1,44 | 1,71 | 1,83 | 1,46 | 1,11 | 2,09 | 1,56 |
| $T_{(liquidus)}$(℃)[3] | 1330 | 1351 | 1340 | 1362 | 1329 | 1345 | 1363 | 1363 | 1346 | 1323 | 1403 | 1371 |

[1] $CaO(wt.\%)/Al_2O_3(wt.\%)$ ; [2] atomic $Mg/(Mg+Fe^{2+})$ ; [3] $1026e^{[0.01894MgO(wt.\%)]}$(℃)(Niu, 2005) ; - : Below detection limit

| Sample | MI13 | MI14 | MI15 | MI16 | MI17 | MI18 | MI19 | MI20 | MI21 | MI22 | MI23 | MI24 |
|---|---|---|---|---|---|---|---|---|---|---|---|---|
| | Pl13 | Pl7 | Pl15 | Pl8 | Pl5 | Pl13 | Pl4 | Pl2 | Pl21 | Pl6 | Pl23 | Pl4 |
| $SiO_2$ | 49,00 | 47,12 | 50,95 | 49,91 | 47,50 | 48,15 | 49,21 | 48,65 | 47,19 | 49,64 | 49,31 | 50,71 |
| $TiO_2$ | 2,33 | 2,35 | 1,04 | 1,17 | 1,84 | 1,79 | 1,64 | 1,75 | 1,97 | 1,55 | 1,69 | 2,05 |
| $Al_2O_3$ | 5,12 | 4,61 | 10,80 | 9,70 | 5,64 | 6,13 | 6,15 | 6,21 | 5,59 | 7,87 | 5,74 | 6,76 |
| FeO | 15,97 | 14,77 | 12,94 | 14,69 | 15,14 | 14,43 | 15,92 | 14,92 | 15,93 | 15,03 | 16,43 | 14,97 |
| MgO | 13,64 | 17,26 | 11,41 | 11,37 | 15,02 | 15,79 | 14,10 | 15,85 | 15,65 | 11,83 | 12,18 | 13,57 |
| MnO | 0,30 | 0,30 | 0,26 | 0,28 | 0,30 | 0,27 | 0,26 | 0,30 | 0,31 | 0,31 | 0,29 | 0,24 |
| CaO | 11,86 | 11,13 | 10,94 | 10,54 | 11,76 | 11,45 | 10,61 | 11,81 | 11,32 | 11,37 | 11,42 | 11,92 |
| $Na_2O$ | 0,61 | 0,55 | 1,28 | 1,19 | 0,37 | 0,36 | 0,46 | 0,54 | 0,54 | 0,50 | 0,69 | 0,43 |
| $K_2O$ | 0,15 | 0,10 | 0,10 | 0,14 | 0,05 | 0,08 | 0,12 | 0,05 | 0,06 | 0,13 | 0,13 | 0,08 |
| $Cr_2O_3$ | 0,17 | 0,13 | 0,06 | 0,07 | 0,28 | 0,12 | 0,17 | 0,22 | 0,10 | 0,14 | 0,12 | 0,07 |
| NiO | - | - | 0,01 | 0,03 | 0,02 | 0,05 | 0,01 | - | 0,02 | 0,03 | 0,02 | - |
| Total | 99,15 | 98,32 | 99,79 | 99,09 | 97,92 | 98,62 | 98,65 | 100,30 | 98,68 | 98,40 | 98,02 | 100,80 |
| Ca/Al[1] | 2,32 | 2,41 | 1,01 | 1,09 | 2,09 | 1,87 | 1,73 | 1,90 | 2,03 | 1,44 | 1,99 | 1,76 |
| Mg#[2] | 0,63 | 0,70 | 0,64 | 0,61 | 0,66 | 0,68 | 0,64 | 0,68 | 0,66 | 0,61 | 0,59 | 0,64 |
| $Ca_{72}/Al_{72}$ | 1,80 | 2,22 | 0,85 | 0,89 | 1,75 | 1,65 | 1,38 | 1,66 | 1,68 | 1,16 | 1,50 | 1,45 |
| $T_{(liquidus)}$(℃)[3] | 1328 | 1423 | 1273 | 1273 | 1364 | 1384 | 1340 | 1385 | 1380 | 1284 | 1292 | 1327 |

[1] $CaO(wt.\%)/Al_2O_3(wt.\%)$ ; [2] atomic $Mg/(Mg+Fe^{2+})$ ; [3] $1026e^{[0.01894MgO(wt.\%)]}$(℃)(Niu, 2005) ; - : Below detection limit

**TABLE 2.** Major element composition of host plagioclases in SMAR19ºS MORB (wt.%)

| Host. | Pl1 | Pl2 | Pl3 | Pl4 | Pl5 | Pl6 | Pl7 | Pl8 | Pl9 | Pl10 | Pl11 | Pl12 | Pl13 | Pl14 | Pl15 |
|---|---|---|---|---|---|---|---|---|---|---|---|---|---|---|---|
| $SiO_2$ | 47,96 | 47,52 | 53,50 | 46,51 | 46,38 | 48,85 | 47,77 | 46,36 | 47,45 | 48,13 | 46,64 | 46,24 | 45,84 | 45,44 | 45,04 |
| $TiO_2$ | 0,03 | 0,03 | - | 0,03 | 0,02 | 0,04 | 0,07 | 0,02 | 0,02 | 0,03 | 0,04 | 0,04 | 0,04 | 0,04 | 0,04 |
| $Al_2O_3$ | 33,42 | 33,60 | 22,81 | 33,62 | 33,83 | 32,03 | 33,03 | 34,23 | 33,49 | 32,67 | 34,20 | 34,52 | 34,84 | 35,17 | 35,49 |
| FeO | 0,34 | 0,32 | 0,32 | 0,33 | 0,64 | 0,42 | 0,41 | 0,39 | 0,37 | 0,36 | 0,32 | 0,42 | 0,37 | 0,33 | 0,35 |
| MgO | 0,21 | 0,17 | 0,36 | 0,22 | 0,25 | 0,23 | 0,24 | 0,25 | 0,30 | 0,27 | 0,28 | 0,28 | 0,29 | 0,30 | 0,30 |
| MnO | - | 0,01 | 0,01 | 0,01 | 0,02 | 0,01 | - | - | - | 0,01 | - | 0,01 | 0,01 | - | 0,01 |
| CaO | 17,02 | 17,31 | 21,69 | 17,83 | 17,54 | 17,44 | 17,68 | 17,65 | 17,39 | 17,51 | 17,56 | 17,61 | 17,66 | 17,71 | 17,77 |
| $Na_2O$ | 1,97 | 1,65 | 1,65 | 1,72 | 1,60 | 1,86 | 1,27 | 1,95 | 1,74 | 1,90 | 1,81 | 1,85 | 1,69 | 1,73 | 1,77 |
| $K_2O$ | 0,01 | 0,01 | 0,02 | 0,03 | 0,04 | 0,01 | 0,01 | 0,01 | 0,02 | 0,02 | 0,01 | 0,01 | 0,03 | 0,02 | 0,01 |
| $Cr_2O_3$ | - | - | 0,02 | 0,01 | 0,01 | 0,03 | - | 0,01 | 0,01 | - | - | 0,01 | 0,01 | - | 0,02 |
| NiO | - | 0,01 | 0,01 | - | 0,01 | - | 0,01 | 0,00 | 0,01 | - | - | 0,01 | 0,01 | - | - |
| Total | 100,96 | 100,63 | 100,39 | 100,31 | 100,34 | 100,92 | 100,49 | 100,87 | 100,80 | 100,90 | 100,86 | 101,00 | 100,79 | 100,74 | 100,80 |
| An[1] | 81,2 | 84 | 86,8 | 83,8 | 84,6 | 82,4 | 87,4 | 81,9 | 83,3 | 82,2 | 82,9 | 82,6 | 83,9 | 83,7 | 83,4 |

[1] 100×atomic Ca/ (Ca + Na + K); -： Below detection limit

and melt inclusions' composition has been carried out to evaluate their potential relationships.

## RESULTS

The major oxide data of representative melt inclusions and plagioclase hosts from SMAR19ºS are given in Table 1 and 2, respectively. The composition of melt inclusions are characterized by variable MgO content (17.26–11.37wt.%) with Mg#[100×atomic $Mg^{2+}/(Mg^{2+}+Fe^{2+})$] ranging from 68 to 57; $Al_2O_3$ and CaO content from 4.61 to 9.7wt.%, and from 10.54 to 12.05wt.%, respectively, with a Ca/Al ratio of 1.0 to 2.5 (Table 1). Ca/Al and Ca/Na in plagioclase-hosted melt inclusions are positively correlated with MgO (Fig.2, gray arrows), showing that melt composition might be modified by PEC. All the analytical data, including those investigated from SMAR19ºS, those taken from the PetDB, as well as those from other literature sources were normalized to 100wt.% before plotting. In the host plagioclase crystals, the range of An is 87.4–81.2mol.% with an average value of 83 (Table 2).

In addition, we selected major oxide compositions of 162 plagioclase-hosted and 70 olivine-hosted melt inclusions from the PetDB, based on the selection criteria of Spreading center → Basalt → Plagioclase/Olivine → Melt inclusion → Unheated in sequence. Data were downloaded from PetDB on 12 June 2014. The compiled data show that plagioclase-hosted melt inclusions have lower CaO and $Al_2O_3$, higher MgO and FeO, higher Ca/Al, and higher Mg# than olivine-hosted melt inclusions (Fig.3). It can be inferred that besides magma evolution, some modification processes have occurred in the plagioclase-hosted melt inclusions increasing their Ca/Al and Mg# up to 1.5 and >75, respectively. For example during the plagioclase PEC process, the decrease of CaO and $Al_2O_3$ stimulates an increase of MgO and FeO in the plagioclase-hosted melt inclusions (Nielsen *et al.*, 1995; Nielsen, 2011).

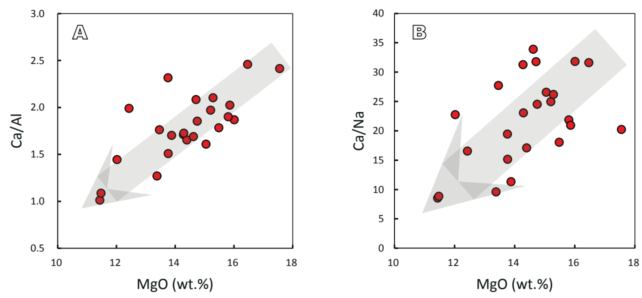


**FIGURE 2.** MgO versus A) Ca/Al and B) Ca/Na in the plagioclase-hosted melt inclusions from SMAR19°S. Gray arrows broadly represent the correlations.

In the plagioclase-hosted melt inclusions from the South-West Indian Ridge (SWIR, data taken from the PetDB) and SMAR19ºS, $Al_2O_3$ is negatively correlated with MgO. This correlation is different from the MORB liquid lines of descent LLD (Fig. 4A, black solid line), but the same as the plagioclase PEC path (Fig. 4A, gray

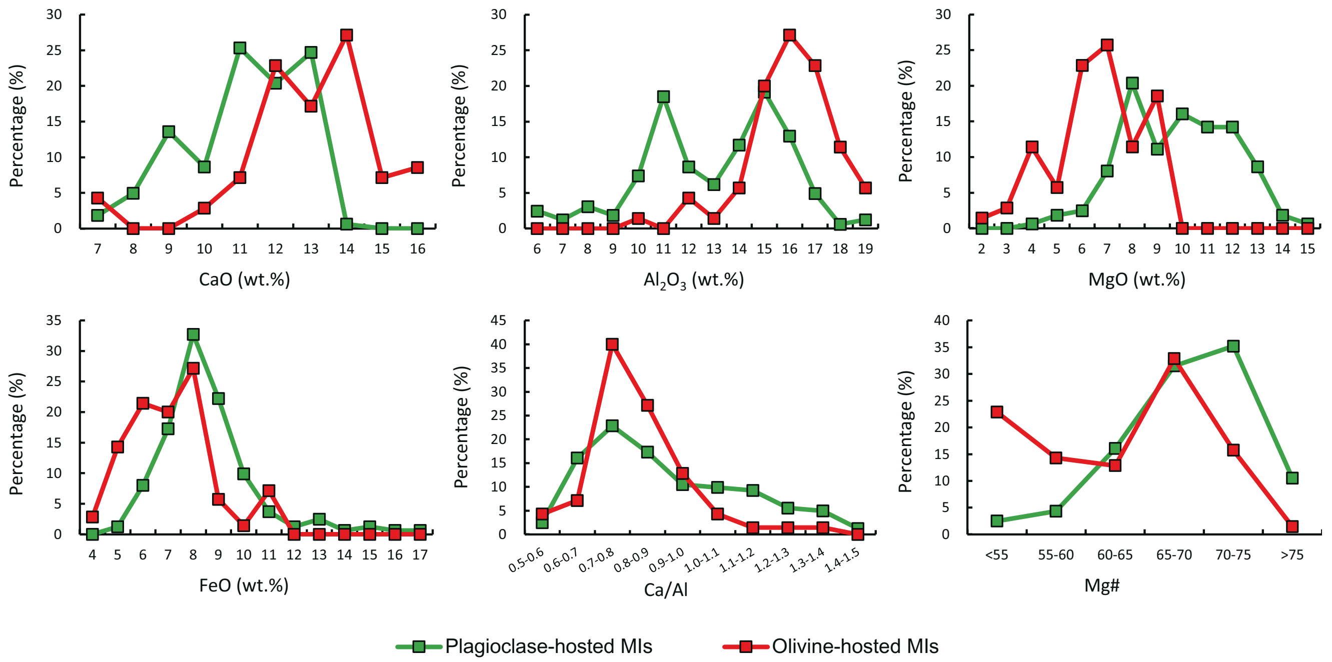


**FIGURE 3.** Comparison of CaO, $Al_2O_3$, MgO, FeO, Ca/Al, and Mg# between olivine (N= 70) and plagioclase-hosted (N= 162) melt inclusions. Data were taken from the PetDB (Lehnert *et al.*, 2000).

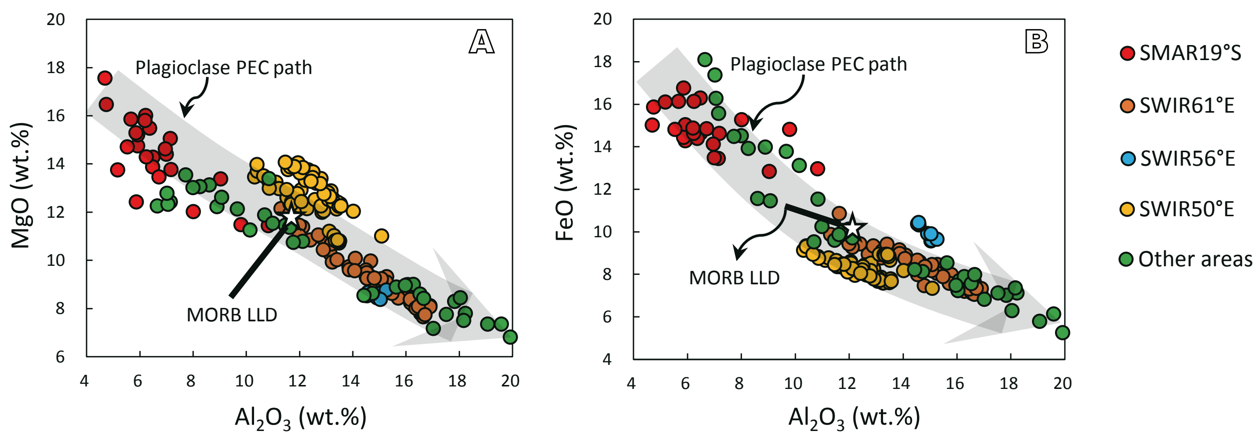


**FIGURE 4.** Plots of $Al_2O_3$ versus A) MgO and B) FeO in plagioclase-hosted MIs from SWIR (Font *et al.*, 2007) and SMAR19°S. The plagioclase PEC path (gray arrows), a hypothetical near-primary melt composition (white stars), and MORB Liquid Lines of Descent (LLD) (black solid lines) are shown for comparison (after Neave *et al.*, 2015).

arrow). On the other hand, the negative correlation between $Al_2O_3$ and FeO is consistent with not only the MORB LLD (Fig.4B, black solid line), but also the plagioclase PEC path (Namur *et al.*, 2011; Neave *et al.*, 2015) (Fig. 4B, gray arrow). This implies that the plagioclase-hosted melt inclusions from the MORB may experience composition modification processes (*e.g.*, PEC). As such this provides an opportunity to find a parameter with wide applicability to assess the composition or modification processes of plagioclase-hosted melt inclusions.

## DISCUSSION

### Fractional crystallization-Ca/Al relationships

Melting cessation beneath ocean ridges may be caused by the increased heat of fusion of residual solid as a result of progressive depletion (Niu and Batiza, 1991), and the effect of pressure-induced solid–solid phase transitions on suppressing melting (Asimow *et al.*, 1995). In addition, conductive cooling and spreading rate are also considered important factors to determine the final extent of melting (Shen and Forsyth, 1995; Niu and Batiza, 1997). However, the partial melts enter the period of fractional crystallization in the Cold Thermal Boundary Layer (CTBL) after melting cessation.

MORBs are anhydrous melts derived from a mantle source region depleted in incompatible elements and volatile components (Niu *et al.*, 1999, 2002). The path of cumulates in anhydrous MORB melt fractionation follows the order of Ol (dunite) → Ol+Pl (troctolite) → Ol+Pl+Cpx (gabbro) (Yoder, 1965; Gaetani, 1993; Niu and Batiza, 1997; Niu *et al.*, 1999, 2002, 2008) (Fig. 5). The effect of dunite crystallization on Ca/Al ratio is insignificant. CaO increases with decreasing MgO during troctolite crystallization and decreases during gabbro crystallization (Fig. 5, green solid line). The $Al_2O_3$ content decreases with increasing extent of magma evolution during troctolite and gabbro crystallization (Fig. 5, blue solid line). Then, the Ca/Al of melt increases during troctolite crystallization (a very short window in terms of temperature, only about 40ºC or less), and reaches a maximum value of ~0.85. Subsequently, the Ca/Al ratio of melt gradually decreases during gabbro crystallization (Fig. 5, red solid line). Therefore, the Ca/Al should not rise above 0.85 at any point during the crystallization of anhydrous MORB

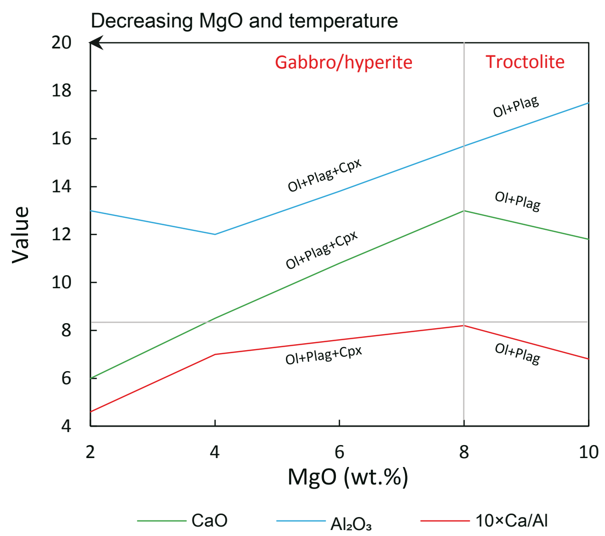


**FIGURE 5.** Liquid Lines of Descent (LLD) illustrated by $Al_2O_3$, CaO and Ca/Al in anhydrous mid-ocean ridge basalt melts (after Niu, 2005; Niu and O'Hara, 2008). The gray vertical continuous line represents the critical point of gabbro/hyperite crystallization at MgO= 8wt.%. The gray horizontal continuous line represents the maximum value of Ca/Al (<0.85) during fractional crystallization processes.

melts. As all melt inclusions in SMAR19ºS have Ca/Al above 1.0, their compositions must have been modified by post-entrapment processes. The same must be true for many plagioclase-hosted melt inclusions from other MORB samples.

### Crystal-melt relationships

During troctolite crystallization (MgO>8wt.%) Ca/Al of residual melt increases with the magma evolution, meaning that high-An plagioclase phenocrysts should entrap melt inclusions with lower Ca/Al. However, by selecting plagioclase-hosted melt inclusions (MIs) with MgO>8wt.% to satisfy the condition that they were entrapped during troctolite crystallization, their Ca/Al is positively correlated with An content (Fig. 6). In order to explain that, let us consider that during the PEC, the host plagioclase absorbs Al and Ca from the melt on the melt inclusion walls. Although the quantity of CaO and $Al_2O_3$ absorbed in the post-entrapment plagioclase crystallization is not remarkable, the Ca/Al in the melt inclusions will change significantly because of their tiny volume (Sobolev and Shimizu, 1993; Sobolev *et al.*, 2000; Danyushevsky *et al.*, 2003, 2004). Considering the molecular formula of anorthite ($Ca[Al_2Si_2O_8]$) and albite ($Na[AlSi_3O_8]$), PEC of melt inclusions in host high-An plagioclase crystals should show greater depletion in $Al_2O_3$ (Nielsen, 2011). In addition, because of the different partition coefficients between CaO and $Al_2O_3$ in plagioclase ($K_{Al}^{Plag}>K_{Ca}^{Plag}$) (Nielsen *et al.*, 1995), host high-An plagioclase phenocrysts will absorb more $Al_2O_3$ from melt inclusions which will make melt inclusions more depleted in $Al_2O_3$, so it will potentially lead melt inclusions to have a higher Ca/Al ratio. The black dashed line area in Figure 6 highlights that for SMAR19ºS plagioclases with An>80, the trend line is very steep (red dashed line with k= 0.21 and $R^2$=0.89). From these relationships it can be inferred that host high-An plagioclase crystals can change the composition of entrapped melt inclusions much easier than host plagioclase crystals with low An content.

### PEC-Ca/Al relationships

According to the sample locations, we have divided the melt inclusions studied by Font *et al.* (2007) into 4 different groups (DR16, DR27, DR28, DR75). Their compositional features are compared to those of SMAR19ºS melt inclusions in the binary diagrams of Figure 7. We find that: i) for melt inclusions with Ca/Al<1.0, MgO is positively correlated with FeO ($R^2$>0.90) (Fig. 7A),and negatively correlated with $Al_2O_3$ ($R^2$>0.88) (Fig. 7B); ii) for melt inclusions with Ca/Al>1.0, like those from SMAR19ºS and the group DR75, the positive correlation between MgO and FeO disappears ($R^2$=0.002) (Fig. 7A), and the negative

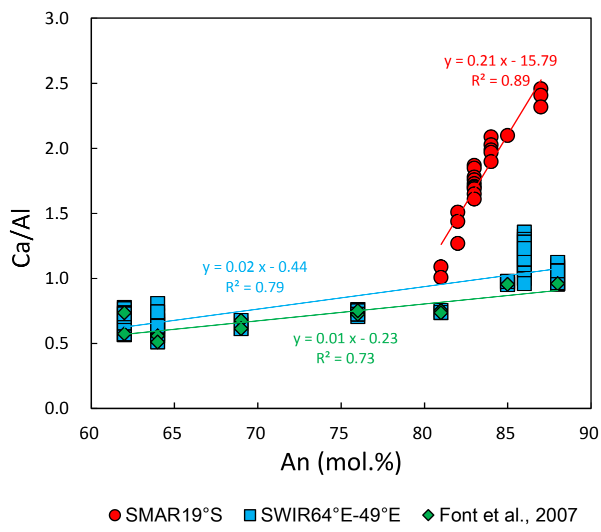


**FIGURE 6.** Correlation between An value of host plagioclase and Ca/Al of melt inclusions with MgO>8wt.%, entrapped during troctolite crystallization. Continuous lines represent the calculated trends.

correlation between MgO and $Al_2O_3$ becomes weaker ($R^2$<0.5) (Fig. 7B). The FeO content is also particularly sensitive to PEC in plagioclase-hosted melt inclusions (Neave *et al.*, 2015). These relationships demonstrate that the composition of melt inclusions with Ca/Al<1.0 was modified by the PEC process. In contrast, for plagioclase-hosted melt inclusions with Ca/Al>1.0, $Al_2O_3$ decreases with increasing MgO, whereas FeO remains substantially unchanged (Fig. 7). This indicates that these melt inclusions were not affected by PEC process, but rather by $Al_2O_3$ depletion processes (*e.g.*, a boundary layer process) (Kent, 2008).

The melt inclusion compositional data taken from the PetDB and tested in this study show that: for plagioclase-hosted melt inclusions with Ca/Al<1.0, at increasing Ca/Al, the $Al_2O_3$ and $Na_2O$ content decrease is following trend lines with slope k=-7.0 ($R^2$=0.27) (Fig. 8A) and k=-6.8 ($R^2$=0.8) (Fig. 8B), respectively, while CaO content increases following a trend line with k=9.2 ($R^2$=0.58) (Fig. 8C). This implies that when Ca/Al<1.0, plagioclase crystallization is the most important post-entrapment process (Namur *et al.*, 2011). In contrast, when Ca/Al>1, at increasing Ca/Al, the $Al_2O_3$, $Na_2O$ and CaO content decreases following a trend line with k= -10.9 ($R^2$=0.62) (Fig. 8A), k= -1.76 ($R^2$=0.32) (Fig. 8B), and k= -2.69 ($R^2$=0.06) (Fig. 8C), respectively. Particularly, melt inclusions from SMAR19ºS have high Ca/Al, in the range of 1.0 to 2.4. At increasing Ca/Al, their $Na_2O$ and CaO content is near-constant, following trend lines with k=-0.50 ($R^2$=0.43) and k=0.59 ($R^2$=0.28), respectively (Fig. 8B, C), while the $Al_2O_3$ content decreases following a trend line with k= -3.8 and a very good correlation ($R^2$= 0.9) (Fig. 8A). These

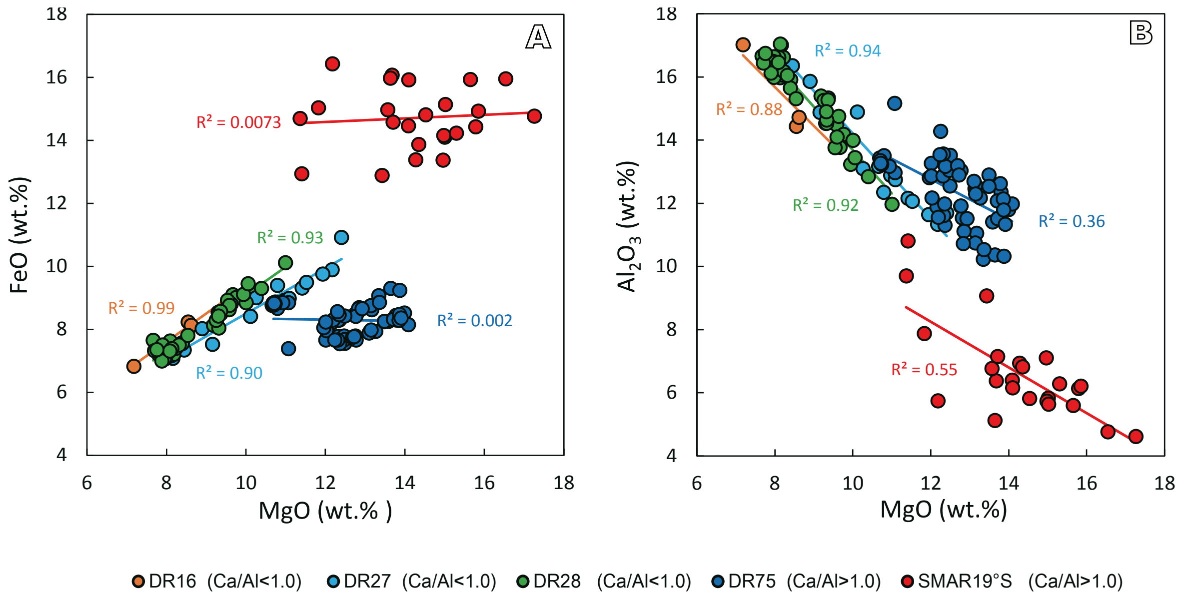


**FIGURE 7.** Plots summarizing the relationships of MgO against A) FeO and B) $Al_2O_3$ in plagioclase-hosted melt inclusions. Continuous lines represent the calculated trend lines in different sampling sites. DR16, DR 27, DR 28, DR 75 sample data were taken from Font *et al.* (2007).

characteristics indicate undoubtedly that melt inclusions with Ca/Al>1 have been modified by some $Al_2O_3$ depletion process besides PEC. Because we were only interested in whether the melt inclusions potentially have the ability to reveal the melt composition at the time of entrapment, more complex modification processes have not been investigated further.

**Original melt - Ca/Al relationships**

A primary MORB melt with Mg#= 72 passing through the Moho is in equilibrium with olivine with $\geq Fo_{89}$ (Niu and O'Hara, 2008). On this basis, more evolved MORB rocks and melt inclusions can be corrected for fractionation to Mg#= 72. Melts corrected to Mg#=72 thus reflect more faithfully mantle signatures or processes. Considering the $Mg\#_{72}$ correction as the inverse process of fractionation, it is certain that $Ca_{72}/Al_{72}$ should be less than the measured Ca/Al [(Ca/Al)/($Ca_{72}/Al_{72}$)>1.0]. $Mg\#_{72}$ correction is applied only to melt inclusion compositions with Mg#<72 and MgO>7wt.%. (Ca/Al)/($Ca_{72}/Al_{72}$) is controlled by Mg# in the correction process (Niu and O'Hara, 2008).

We corrected plagioclase-hosted melt inclusion compositions of Font *et al.* (2007) to Mg#=72 for fractionation effects. The correction shows that melt inclusions with Ca/Al<0.78, have Mg# and (Ca/Al)/($Ca_{72}/Al_{72}$) less than 0.72 and greater than 1.0 (about 1.05~1.20), respectively (Fig. 9). This demonstrates that the composition of melt inclusions with Ca/Al<0.78 is consistent with magma evolution characteristics, and can be effectively corrected for fractionation effects to Mg#=72. On the other hand, 88% of the melt inclusions with Ca/Al>0.78 selected from the PetDB with Mg#>72 cannot be corrected, and have (Ca/Al)/($Ca_{72}/Al_{72}$)<1.0. Conversely, melt inclusions with Mg#<72 and (Ca/Al)/($Ca_{72}/Al_{72}$)>1.0 are similar to those tested in this study. Calculated liquidus temperatures for melt inclusions from SMAR19ºS are in the range of 1270ºC (MgO=11.37wt.%) to 1403ºC (MgO=17.26wt.%) (Fig.10, Table 1). This suggests temperatures of 1270–1400ºC for plagioclase fractional crystallization, which are obviously higher than the temperature (<1250ºC) for phase equilibrium in plagioclase phenocrysts-bearing anhydrous tholeiitic basalts (Sobolev *et al.*, 1988). The liquidus temperature is positively correlated with Ca/Al ($R^2$=0.55) (Fig.10), which suggests that melt inclusions with higher Ca/Al will have a higher MgO, and may have been modified to a greater extent (Fig. 10). Therefore, the compositions of melt inclusions with Ca/Al>0.78 cannot be restored to their original composition by using the $Mg\#_{72}$ correction.

As shown in Figure 9, there is an abrupt increase in Mg# and Ca/Al when An is greater than 80. Despite that the reason for this sharp increase remains unclear, our study potentially demonstrates that Ca/Al is a reliable indicator of whether or not melt inclusions in MORB samples have been modified by PEC or other post-entrapment processes: i) melt inclusions with Ca/Al<1 have been mostly modified by PEC; ii) those with Ca/Al<0.78 can be restored to their original composition when corrected by Mg#=72. However, it is noteworthy

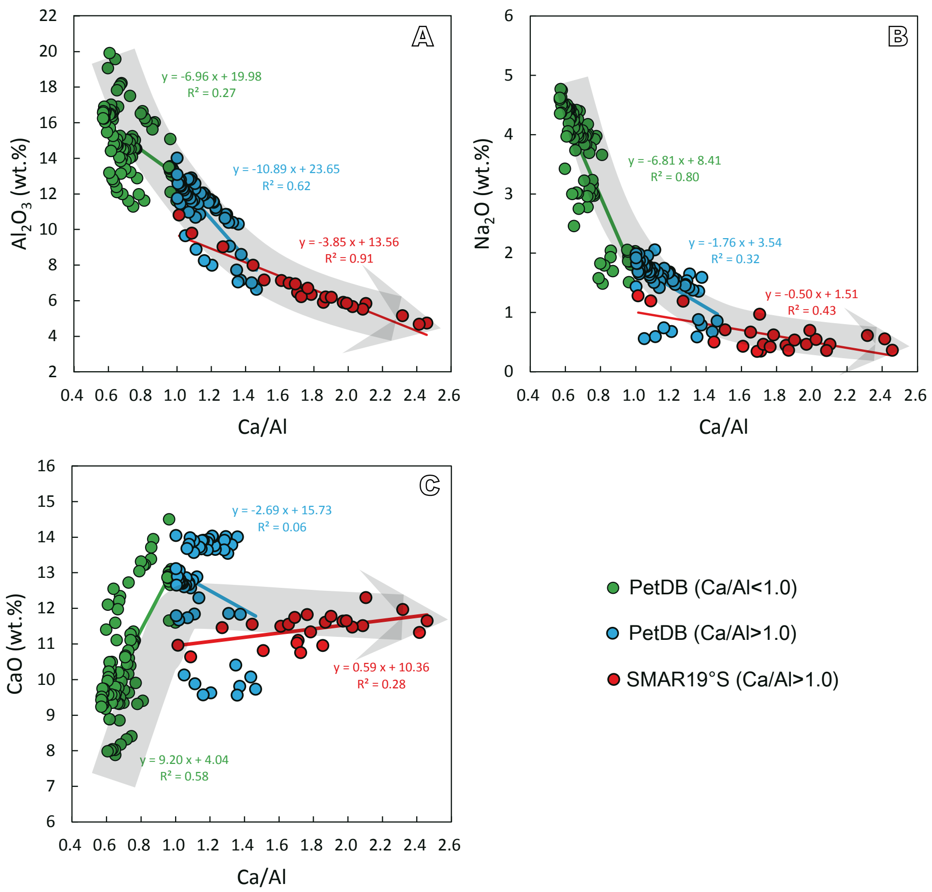


**FIGURE 8.** Variations of A) $Al_2O_3$, B) $Na_2O$ and C) CaO with increasing Ca/Al. Continuous lines represent the calculated trend lines of sample data with different Ca/Al. Gray arrows represent the variability of trend sin data. Except for SMAR19°S data were taken from the PetDB (Lehnert *et al.*, 2000).

that Ca/Al cannot precisely indicate all modification processes experienced by the melt inclusions, because of the differences in source regions and magmatic evolution. When the relationships between $Al_2O_3$, MgO, FeO, CaO, $Na_2O$, Mg# and Ca/Al are simultaneously taken into account, Ca/Al can be regarded as a reliable indicator of whether melt inclusions reflect the original melt composition. Application of this indicator to other case studies would be desirable in order to better assess its reliability.

## CONCLUSIONS

i) Post-entrapment crystallization of plagioclase-hosted melt inclusions leads to negative correlations between FeO, MgO and $Al_2O_3$. Plagioclase-hosted melt inclusions tend to have higher Ca/Al, Mg#, MgO, FeO content, and lower CaO and $Al_2O_3$ content than melt inclusions hosted in olivine.

ii) Ca/Al is a diagnostic indicator of whether or not plagioclase-hosted melt inclusions can represent the original melt composition. When Ca/Al<0.78, the melt inclusions corrected for fractionation effects to Mg#=72 can represent the primary melt. When 0.78<Ca/Al<1.0, melt inclusions are mainly modified by post-entrapment

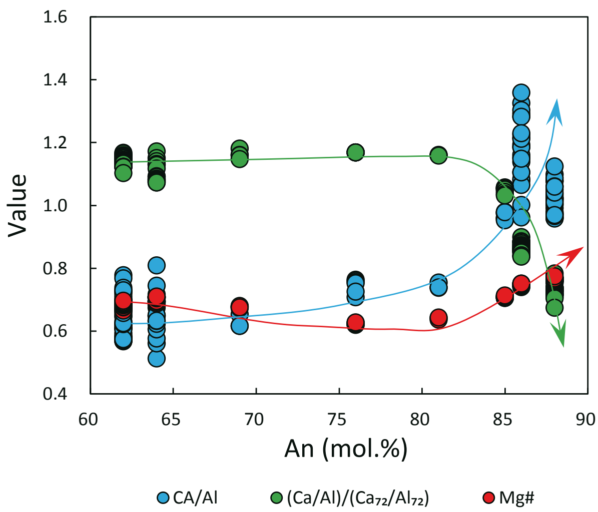


**FIGURE 9.** Variations of Ca/Al, $(Ca/Al)/(Ca_{72}/Al_{72})$ and Mg# with increasing An content in host plagioclases. Continuous curves represent the general variability trends.

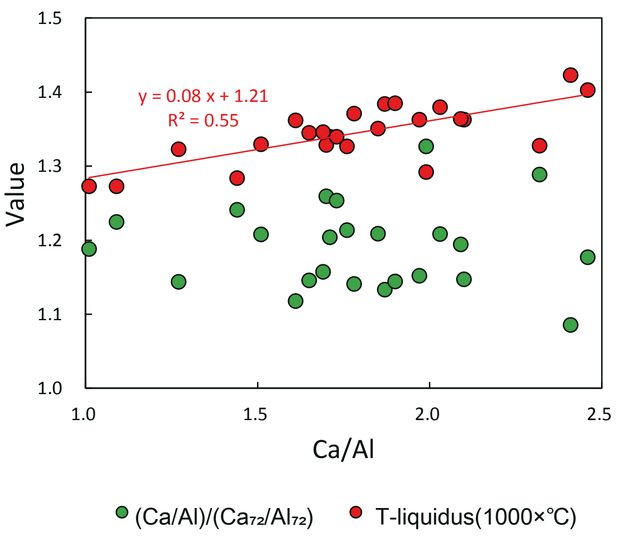


**FIGURE 10.** Variations of T-liquidus and (Ca/Al)/($Ca_{72}$/$Al_{72}$) with increasing Ca/Al. The red continuous line represents the calculated trend line of T-liquidus.

plagioclase crystallization, and can reveal the original melt composition after PEC correction. When Ca/Al>1.0, the melt inclusion composition cannot be restored to reflect the original melt or mantle source composition. So, in SMAR19ºS MORB, plagioclase-hosted melt inclusions with Ca/Al>1.0 cannot represent the composition of the melt at the moment of their entrapment.

## ACKNOWLEDGEMENTS

The authors gratefully acknowledge the financial support of China Ocean Mineral Resources R&D Association Project (DY125-12-R-01), International Cooperation Ministry of Science and Major Projects (2006DFB21620), and National Natural Science Foundation of China (41322036, 41576052). We are indebted to all of the scientists of China Ocean Survey (COS) Expedition nº 22, and the contributors of Petrological Database (PetDB). Thanks to LI B. and DONG W.D. for assistance in the analysis of the samples. Discussions with NIU Y.L.,LU H.Z. and MENG X.W. were helpful, and reviews by Dr. Margaret Hartley, Dr. Paola Marianelli and the editor Prof. Massimo D'Antonio greatly improved the clarity and focus of the manuscript.

## REFERENCES

Asimow, P.D., Hirschmann, M.M., Ghiorso, M.S., 1995. The effect of pressure-induced solid-solid phase transitions on decompression melting of the mantle. Geochimica et Cosmochimica Acta, 59, 4489-4506.

Baker, D.R., 2008. The fidelity of melt inclusions as records of melt composition. Contributions to Mineralogy and Petrology, 156(3), 377-395.

Cottrell, E., Spiegelman, M., Langmuir, C.H., 2002. Consequences of diffusive re-equilibration for the interpretation of melt inclusions. Geochemistry, Geophysics, Geosystems, 3(5), 1-26. DOI: 10.1029/2001GC000205.

Danyushevsky, L.V., Della-Pasqua, F.N., Sokolov, S., 2000. Re-equilibration of melt inclusions trapped by magnesian olivine phenocrysts from subduction-related magmas: petrological implications. Contributions to Mineralogy and Petrology, 138, 68-83.

Danyushevsky, L.V., McNeill, A.W., Sobolev, A.V., 2002. Experimental and petrological studies of melt inclusions in phenocrysts from mantle-derived magmas: an overview of techniques, advantages and complications. Chemical Geology, 183, 5-24.

Danyushevsky, L.V., Perfit, M.R., Eggins, S.M., Falloon, T.J., 2003. Crustal origin for coupled 'ultra-depleted' and 'plagioclase' signatures in MORB olivine-hosted melt inclusions: evidence from the Siqueiros Transform Fault, East Pacific Rise. Contributions to Mineralogy and Petrology, 144, 619-637.

Danyushevsky, L.V., Leslie, R.A.J., Crawford, A.J., Durance, P., 2004. Melt inclusions in primitive olivine phenocrysts: The role of localized reaction processes in the origin of anomalous compositions. Journal of Petrology, 45, 2531-2553.

Demets, C., Gordon, R. G.D., Argus, F., Stein, S., 1994. Effect of recent revisions to the geomagnetic reversal time scale on estimates of current plate motions, Geophysical Research Letters, 21(20), 2191–2194.

Dungan, M.A., Rhodes, J.M., 1978. Residual glasses and melt inclusions in basalts from DSDP Legs 45 and 46 evidence for magma mixing. Contributions to Mineralogy and Petrology, 67, 417-431.

Faure, F., Schiano, P., 2005. Experimental investigation of equilibration conditions during forsterite growth and melt inclusion formation. Earth and Planetary Science Letters, 236, 882-898.

Font, L., Murton, B.J., Roberts, S., Tindle, A.G., 2007, Variations in melt productivity and melting conditions along SWIR (70 degrees E-49 degrees E): evidence from olivine-hosted and plagioclase-hosted melt inclusions. Journal of Petrology, 48, 1471-1494.

Gaetani, G.A., Grove, T.L., Bryan, W.B., 1993. The influence of water on the petrogenesis of subduction-related igneous rocks. Nature, 365, 332-334.

Gaetani, G.A., Watson, E.B.,2000. Open-system behavior of olivine-hosted melt inclusions. Earth and Planetary Science Letters, 183, 27-41.

Hansen, H., Gronvold, K.,2000. Plagioclase ultraphyric basalts in Iceland: the mush of the rift. Journal of Volcanology and Geothermal Research, 98, 1-32.

Hartley, M.E., Thordarson, T., 2013. The 1874–1876 volcano-tectonic episode at Askja, North Iceland: Lateral flow revisited. Geochemistry, Geophysics, Geosystems, 14(7), 2286-2309.

Hartley, M.E., Thordarson, T., Fitton, J.G., 2013. Oxygen isotopes in melt inclusions and glasses from the Askja volcanic system, North Iceland. Geochimica et Cosmochimica Acta, 123, 55-73.

Kamenetsky, V.S., Eggins, S.M., Crawford, A.J., Green, D.H., Gasparon, M., Falloon, T.J., 1998. Calcic melt inclusions in primitive olivine at 43ºN MAR: evidence for melt-rock reaction/melting involving clinopyroxene-rich lithologies during MORB generation. Earth and Planetary Science Letters, 160, 115-132.

Kent, A.J.R., 2008. Melt inclusions in basaltic and related rocks. Reviews in Mineralogy & Geochemistry, 69, 273-331.

Laubier, M., Schiano, P., Doucelance, R., Ottolini, L., Laporte, D., 2007. Olivine-hosted melt inclusions and melting processes beneath the FAMOUS zone (Mid-Atlantic Ridge). Chemical Geology, 240, 129-150.

Lehnert, K., Su Y., Langmuir C.H., Sarbas, B., Nohl, U., 2000. A global geochemical database structure for rocks, Geochemistry, Geophysics, Geosystems, 1, 1012.

Namur, O., Charlier, B., Toplis, M., Vander-Auwera, J., 2011. Prediction of plagioclase-melt equilibria in anhydrous silicate melts at 1-atm. Contributions to Mineralogy and Petrology, 163,133-150. DOI:10.1007/s00410-011-0662-z

Neave, D.A., Passmore, E., Maclennan, J., Fitton, G., Thordarson, T., 2013. Crystal-melt relationships and the record of deep mixing and crystallization in the AD 1783–84 Laki eruption, Iceland. Journal of Petrology, 54, 1661-1690. DOI:10.1093/petrology/egt027

Neave, D.A., Maclennan, J., Hartley, M.E., Edmonds, M., Thordarson, T., 2014. Crystal storage and transfer in basaltic systems: the Skuggafjöll eruption, Iceland. Journal of Petrology, 55, 2311-2356. DOI:10.1093/petrology/egu058

Neave, D.A., Maclennan, J., Thordarson, T., Hartley, M.E., 2015. The evolution and storage of primitive melts in the Eastern Volcanic Zone of Iceland: the 10 ka Grímsvötn tephra series (*i.e.* the Saksunarvatn ash). Contributions to Mineralogy and Petrology, 170(2), 1-23.

Nielsen, R.L., 2011. The effects of the re-homogenization on plagioclase hosted melt inclusions. Geochemistry, Geophysics, Geosystems, 12(10), 1241-1249. DOI:10.1029/2011GC003822

Nielsen, R.L., Crum, J., Bourgeois, R., Hascall, K., Forsythe, L.M., Fisk, M.R., Christie, D.M., 1995. Melt inclusions in high-An plagioclase from the Gorda Ridge: an example of the local diversity of MORB parent magmas. Contributions to Mineralogy and Petrology, 122, 34-50.

Niu, Y.L., Batiza, R., 1991. An empirical method for calculating melt compositions produced beneath mid-ocean ridges: application for axis and off-axis (seamounts) melting. Journal of Geophysical Research, 96, 21753-21777.

Niu, Y.L., Batiza, R., 1997. Trace element evidence from seamounts for recycled oceanic crust in the eastern Pacific mantle. Earth and Planetary Science Letters, 148, 471-483.

Niu, Y.L., O'Hara, M.J., 2008. Global correlations of ocean ridge basalt chemistry with axial depth: A new perspective. Journal of Petrology, 49, 633-664.

Niu, Y.L., Collerson, K.D., Batiza, R., Wendt, J.I., Regelous, M., 1999. The origin of E-Type MORB at ridges far from mantle plumes: The East Pacific Rise at 11º20′N. Journal of Geophysical Research, 104, 7067-7087.

Niu, Y.L., Regelous, M., Wendt, J.I., Batiza, R., O'Hara, M.J., 2002. Geochemistry of near-EPR seamounts: Importance of source vs. process and the origin of enriched mantle component. Earth and Planetary Science Letters, 199, 329-348.

Portnyagin, M., Almeev.R., Matveev, S., Holtz, F., 2008. Experimental evidence for rapid water exchange between melt inclusions in olivine and host magmas. Earth and Planetary Science Letters, 272, 541-552.

Qin, Z., Lu, F., Anderson, A.T.J., 1992. Diffusive re-equilibration of melt and fluid inclusions. American Mineralogist, 77, 565-576.

Shen, Y., Forsyth, D.W., 1995. Geochemical constraints on initial and final depth of melting beneath mid-ocean ridges. Journal of Geophysical Research, 100, 2211-2237.

Shimizu, N., 1998. The geochemistry of olivine-hosted melt inclusions in a FAMOUS basalt ALV519-4-1. Physics of the Earth and Planetary Interiors, 107, 183-201.

Sinton, C.W., Christie, D.M., Coombs, V.L., Nielsen, R.L., Fisk, M.R., 1993. Near-primary melt inclusions in anorthite phenocrysts from the Galapagos Platform. Earth and Planetary Science Letters, 119, 527-537.

Sobolev, A.V., Shimizu, N., 1993. Ultra-depleted primary melt included in an olivine from the Mid-Atlantic ridge. Nature, 363, 151-154.

Sobolev, A.V., Danyushevsky, L.V., Dmitriev, L.V., Sushchevskaya, N.M., 1988. High-Alumina Magnesium Tholeiite as One of Primary Melts of Basalts of the Mid-Oceanic Ridges. Geokhimiya, (10): 1522-1528.

Sobolev, A.V., Hofmann, A.W., Nikogosian, I.K., 2000. Recycled oceanic crust observed in 'ghost plagioclase' within the source of Mauna Loa lavas. Nature, 404, 986-990.

Sours-Page, R., Johnson, K.T.M., Nielsen, R.L., Karsten, J.L., 1999. Local and regional variation of MORB parent magmas: Evidence from melt inclusions from the Endeavour Segment of the Juan de Fuca Ridge. Contributions to Mineralogy and Petrology, 134, 342-363.

Sours-Page, R., Nielsen, R.L., Batiza, R., 2002. Melt inclusions as indicators of parental magma diversity on the northern East Pacific Rise. Chemical Geology, 183, 237-261.

Spandler, C., O'Neill, H.S.C., Kamenetsky, V.S., 2007. Survival times of anomalous melt inclusions from element diffusion in olivine and chromite. Nature, 447, 303-306.

Tait, S., 1992. Selective preservation of melt inclusions in igneous phenocrysts. American Mineralogist, 77, 146-155.

Yoder, H.S., 1965. Diopside-anorthite-water at five and ten kilobars and its bearing on explosive volcanism. Carnegie Institution of Washington Yearbook, 64, 82-89.

**Manuscript received April 2014;**
**revision accepted October 2015;**
**published Online January 2016.**